

## Supporting Information

### **Encapsulating mesoporous metal nanoparticles: Towards a highly active and stable nanoreactor for oxidative coupling reactions in water**

Houbing Zou,\* Jinyu Dai and Runwei Wang\*

Prof. H. B. Zou  
School of Chemistry and Chemical Engineering  
Shanxi University  
Wucheng Road 92, Taiyuan 030006, P. R. China  
E-mail: zouhb@sxu.edu.cn

Prof. H. B. Zou, Dr. J. Y. Dai, Prof. R. W. Wang  
State Key Laboratory of Inorganic Synthesis and Preparative Chemistry  
College of Chemistry  
Jilin University  
2699 Qianjin Street, Changchun, 130012, P. R. China  
E-mail: rwwang@jlu.edu.cn

## Experimental Section

**Chemicals.** Cetyltrimethylammonium bromide (CTAB, 99.0 %), tetraethylorthosilicate (TEOS, 98%), aqueous ammonia ( $\text{NH}_3 \cdot \text{H}_2\text{O}$ , 25–28%), poly(vinyl pyrrolidone) (PVP, MW $\approx$ 55000) and sodium borohydride ( $\text{NaBH}_4$ , 99.9%) were purchased from Sinopharm Chemical Reagent Co. Ltd. Ascorbic acid ( $\text{C}_6\text{H}_8\text{O}_6$ , AA, 99.9%), 1,4-bis(triethoxysilyl)benzene (BTEB, 96%) and hexadecylpyridinium chloride monohydrate (HDPC, 99.0-102%) were obtained from Sigma-Aldrich. Gold(III) chloride trihydrate ( $\text{HAuCl}_4 \cdot 3\text{H}_2\text{O}$ , >99%), sodium tetrachloropalladate ( $\text{Na}_2\text{PdCl}_4$ , >99%), chloroplatinic acid ( $\text{H}_2\text{PtCl}_6 \cdot 6\text{H}_2\text{O}$ , >99%), rhodium(III) chloride hydrate ( $\text{RhCl}_3 \cdot n\text{H}_2\text{O}$ , Rh $\geq$ 39.5%) and all alcohols were purchased from Aladdin. All chemicals were used as received without any further purification.

### **Synthesis of the Assembled-multisites Nanoreactor YS-mesoPd@PMO, YS-mesoPt@PMO and YS-mesoRh@PMO**

The assembled-multisites nanoreactor YS-mesoPd@PMO was obtained via a “ship in bottle” growth of mesoporous Pd nanoparticles within the amphiphilic hollow Au@PMO nanospheres that were prepared according to our previous reports.<sup>1</sup> In a typical synthesis, 200 mg of Au@PMO nanospheres were dispersed in a mixture containing 36 mL of  $\text{H}_2\text{O}$  and 180 mg of HDPC by ultrasonication. After the addition of  $\text{Na}_2\text{PdCl}_4$  aqueous solution (35.5 mM, 4.5 mL) and stirring at 50 °C for 30 min, 6.0 mL of fresh AA solution (0.1 M) was dropwise added into the mixture. The catalyst YS-mesoPd@PMO was collected by centrifugation after reacting for 3 h and then washed with water and ethanol several times. The surfactant HDPC was removed by refluxing the sample in 100 mL of acidic ethanol for 6 h.

Based-on this facile “ship in bottle” growth strategy, using different metal precursors and surfactants (structure-directing agents) could introduce different mesoporous metal nanoparticles into the amphiphilic hollow Au@PMO nanospheres. The nanoreactor YS-mesoPt@PMO was obtained when using the  $\text{H}_2\text{PtCl}_6$  and CTAB as the metal precursor and the structure-directing agent, respectively. The nanoreactor YS-mesoRh@PMO was obtained when using the  $\text{RhCl}_3$  and CTAB as the metal precursor and the structure-

directing agent, respectively.

### ***Synthesis of the Single-site Nanoreactor YS-ssPd@PMO and the Multi-sites Nanoreactor YS-msPd@PMO***

The single-site nanoreactor YS-ssPd@PMO was prepared according to the same method for the sample YS-mesoPd@PMO except without using the surfactant HDPC. The multi-sites nanoreactor YS-ssPd@PMO was prepared via a simple impregnation-reduction route. Typically, 200 mg of PMO hollow nanospheres were dispersed in 40 mL of H<sub>2</sub>O by ultrasonication. After the addition of Na<sub>2</sub>PdCl<sub>4</sub> aqueous solution (35.5 mM, 4.5 mL), the resultant mixture was stirred for 2 h at room temperature. The solvent was removed by rotary evaporation, and the obtained solid material was transferred to hydrogen atmosphere and heated for 2 h at 200 °C, presenting the multi-sites nanoreactor YS-ssPd@PMO.

### **Materials Characterization**

Scanning electron microscope (SEM) images was performed on a JEOL JSM-6700F field-emission electron microscope. Transmission electron microscopy (TEM), high-angle annular dark-field scanning transmission electron microscopy (HAADF-STEM) images, and energy-dispersive X-ray spectroscopy (EDX) analyses were collected on an FEI Tecnai G<sup>2</sup> F20s-twin D573 field emission transmission electron microscope with an accelerating voltage of 200 kV. Powder XRD patterns were obtained by using a Rigaku 2550 diffractometer with Cu K $\alpha$  radiation ( $\lambda=1.5418$  Å). N<sub>2</sub> adsorption-desorption isotherms were obtained at -196 °C on a Micromeritics ASAP 2010 sorptometer. Samples were degassed at 120 °C for 12 h prior to analysis. Brunauer–Emmett–Teller (BET) surface areas were calculated from the linear part of the BET plot. The pore size distribution was estimated from the adsorption branch of the isotherm by the BJH method. Inductively coupled plasma mass spectrometry (ICP) analyses were carried out on a NexION 350 ICP-MS instrument. The FT-IR spectra were acquired using a Bruker IFS 66 V/SFTIR spectrometer in the range 400-4000 cm<sup>-1</sup>. <sup>29</sup>Si CP-MAS NMR measurements were performed on a Bruker AVANCE III 400 WB spectrometer. The spinning rate was 12 kHz

and a total number of 20000 scans were recorded with 6 s recycle delay for each sample.  $^{13}\text{C}$ -MAS NMR measurements were performed on Varian Infinity Plus 400 NMR spectrometer. The spinning rate was 4 kHz and a total number of 800 scans were recorded with 4 s recycle delay for each sample. XPS analysis was carried out on an ESCALAB 250 X-ray photoelectron spectrometer with Al K $\alpha$  as the excitation source.

## Catalytic Tests

Typically, 0.5 mmol of alcohol, palladium catalysts (1.5 mol %), 1.5 mmol of  $\text{K}_2\text{CO}_3$  (3 equi), 3.5 mL of  $\text{H}_2\text{O}$  and 0.5 mL of ketone were mixed in a 25 mL round flask equipped with a reflux condenser and a magnetic stirrer. The reaction was performed at 80 °C in an oil bath with magnetic stirring (stirring rate: 1000 r.p.m.) for a given time. When the reaction finished, the reaction mixture was acidized with 36% HCl and extracted by  $\text{CH}_2\text{Cl}_2$  for 3 times. The liquid phase was subsequently analyzed by gas chromatography-mass spectrum Shimadzu GCMS-QP2010 Plus with a flame ionization detector (FID), and dodecane was used as an internal standard. The column was GsBP-1ms (30 m); the initial temperature was 50 °C, the heating rate was 5~30 °C /min, and the final temperature was 280 °C, the temperature of FID detector was 250 °C.

For the recycling test, the catalyst was collected by centrifugation after reaction. The residual catalyst was washed with water and ethanol for several times and used directly for the next catalytic reaction.

## Supplementary Figures and Legends

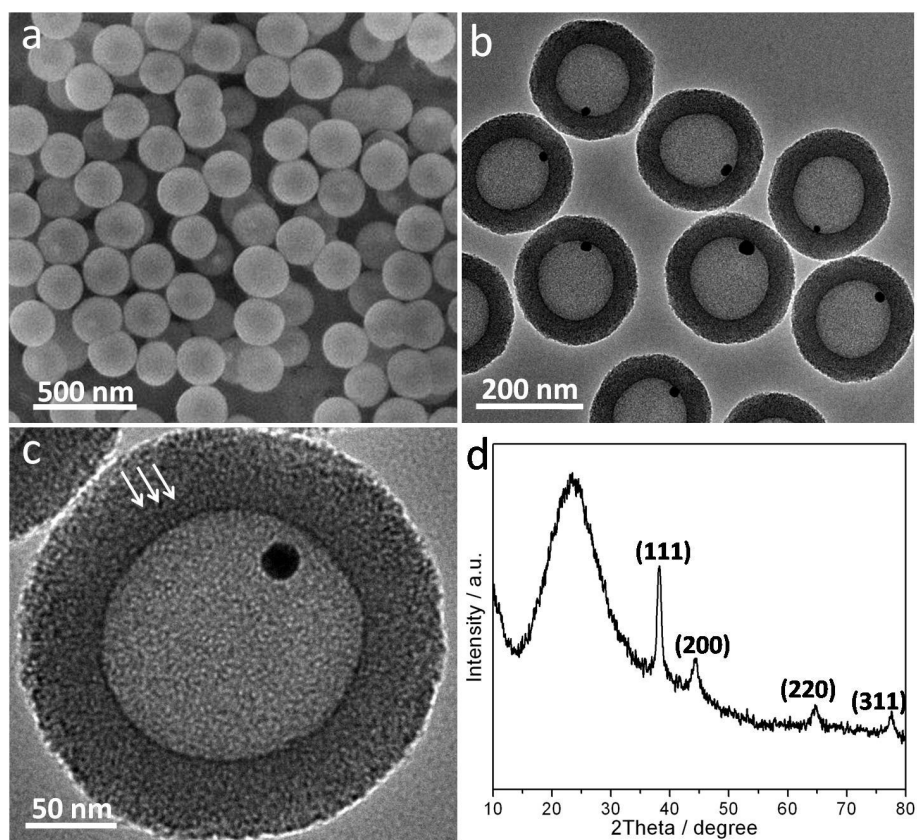


**Figure S1.** SEM image (a), TEM images (b-c) and XRD pattern (d) of unactive Au@PMO hollow nanospheres.

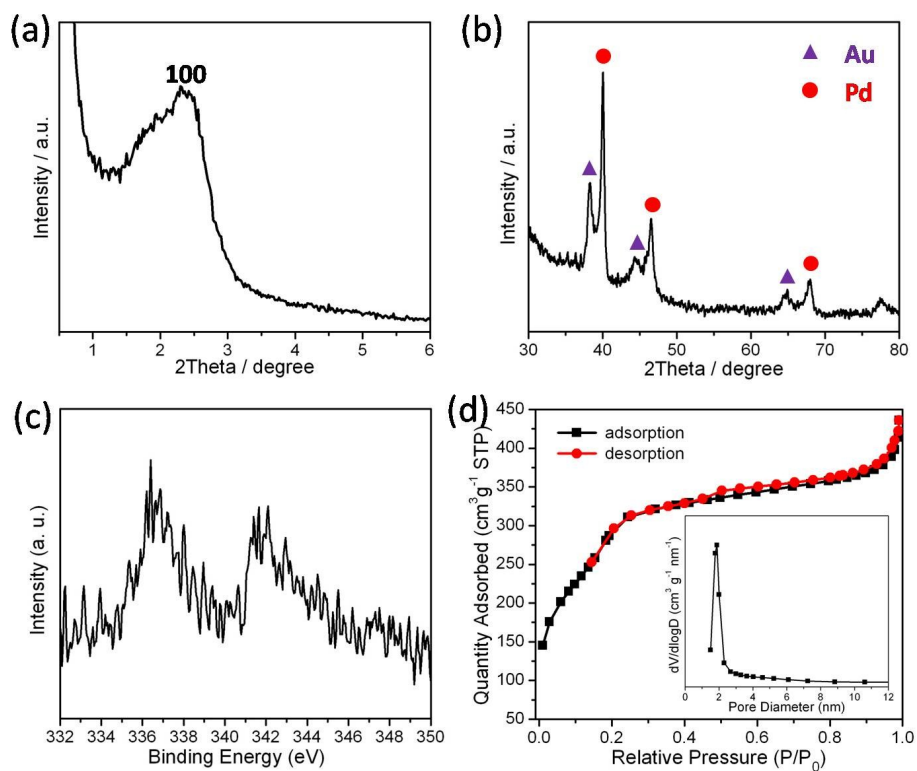


**Figure S2.** Small-angle XRD pattern (a), wide-angle XRD pattern (b), Pd XPS spectrum (c), nitrogen adsorption–desorption isotherm (d) and pore size distribution plot (the inset in d) of the assembled-multisites nanoreactor YS-*meso*Pd@PMO.

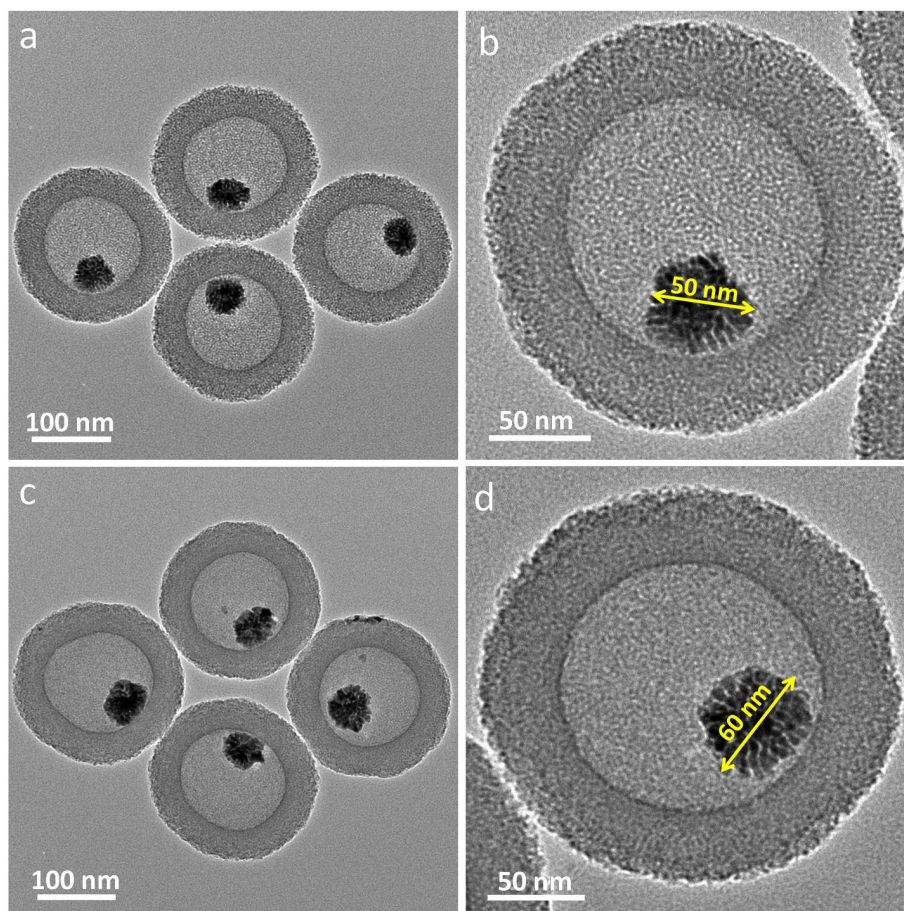


**Figure S3.** Low- and high-magnification TEM images of the assembled-multisites nanoreactor YS-*meso*Pd@PMO with different metal loading: 9.6 wt% (a-b) and 14.5 wt% (c-d).

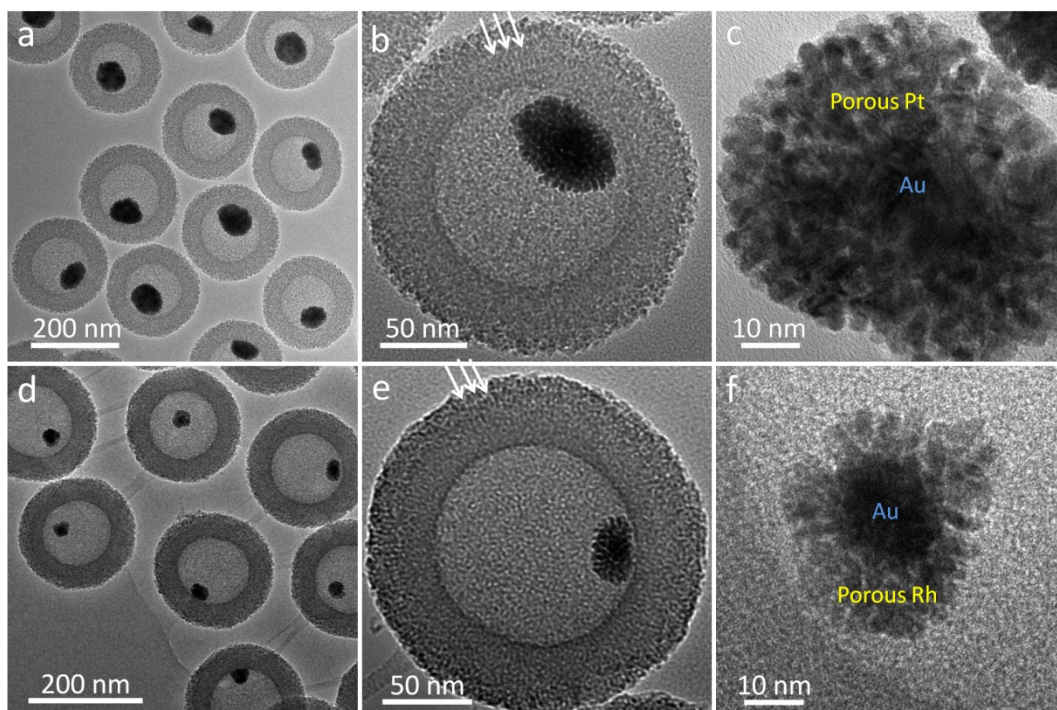


**Figure S4.** Low- and high-magnification TEM images of different assembled-multisites nanoreactor prepared with different metal precursors and structure-directing agents: (a-c) YS-*meso*Pt@PMO, (d-f) YS-*meso*Rh@PMO.

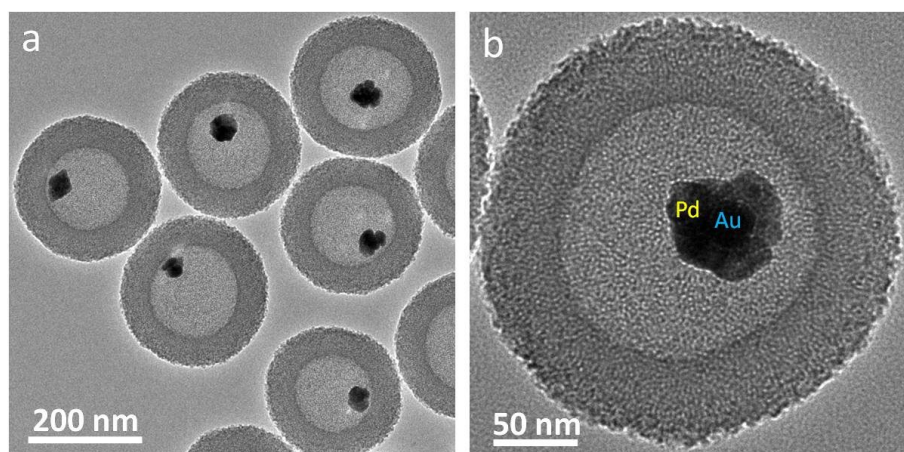


**Figure S5.** TEM images of the single-site nanoreactor YS-ssPd@PMO.



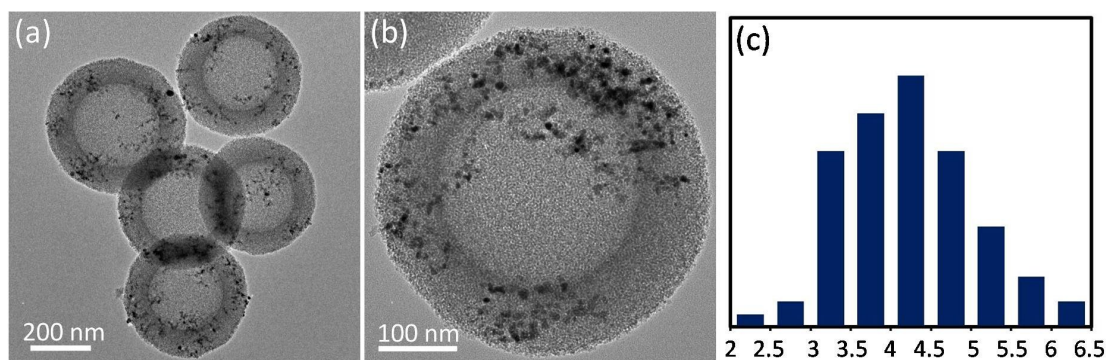


**Figure S6.** (a, b) TEM images of the multi-sites nanoreactor YS-*ms*Pd@PMO. (c) Particle size distribution of the corresponding Pd NPs.

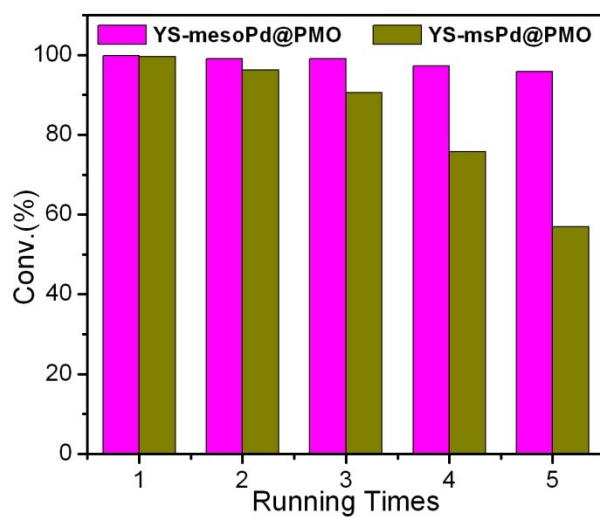


**Figure S7.** Stability tests for the aerobic oxidative coupling of 4-methoxybenzyl alcohol and acetone catalyzed by the catalyst YS-*meso*Pd@PMO and YS-*ss*Pd@PMO.

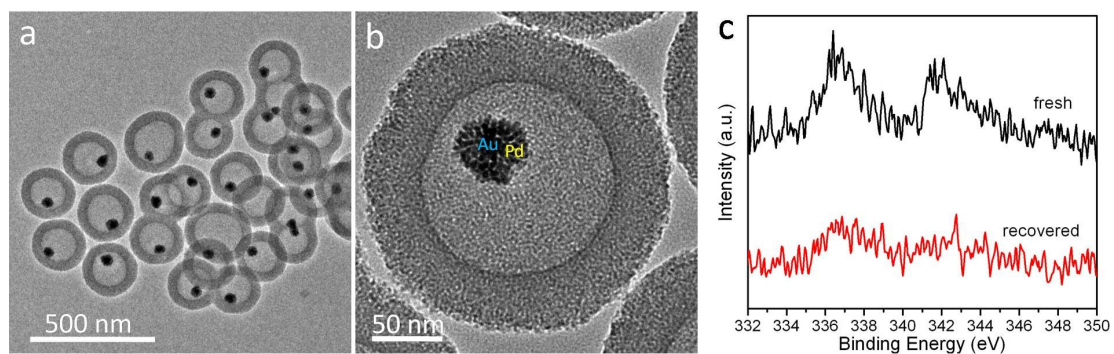


**Figure S8.** TEM images (a, b) and Pd XPS spectrum (c) of the recovered catalyst YS-*meso*Pd@PMO.

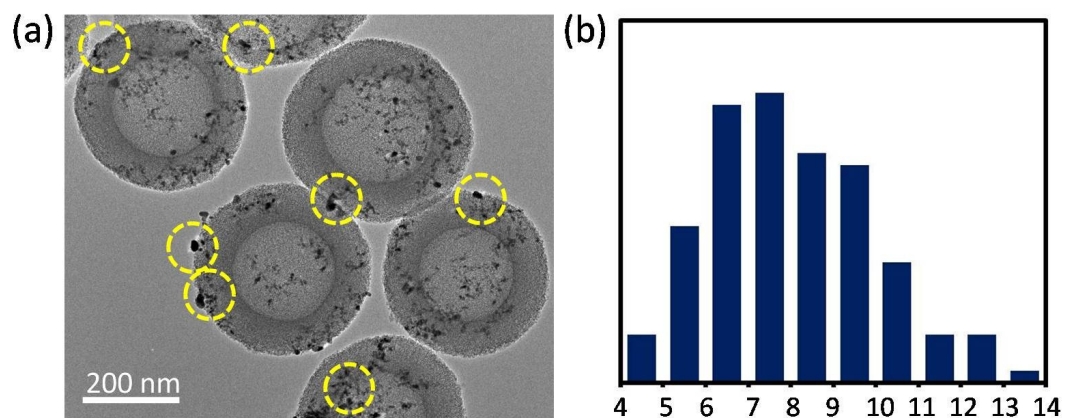


**Figure S9.** (a) TEM image of the recovered multi-sites nanoreactor YS-*ms*Pd@PMO. (b) Particle size distribution of the corresponding Pd NPs.

## References

1. H. B. Zou, R. W. Wang, J. Y. Dai, Y. Wang, X. Wang, Z. T. Zhang and S. L. Qiu, *Chem. Commun.*, 2015, **51**, 1461–1464.